Convective boiling of R-134a and R-123 on an enhanced tube bundle with standard pitch, RP-1316

Evraam Gorgy, Steven Eckels

Published Version Information

Citation: Gorgy, E., & Eckels, S. (2013). Convective boiling of R-134a and R-123 on an enhanced tube bundle with standard pitch, RP-1316. HVAC&R Research, 19(2), 193-206.

Digital Object Identifier (DOI): doi:10.1080/10789669.2012.754308

Publisher's Link: http://www.tandfonline.com/doi/full/10.1080/10789669.2012.754308

Convective Boiling of R-134a and R-123 on an Enhanced Tube Bundle with Standard Pitch, RP-1316

Evraam Gorgy,[1,*] Steven Eckels,[2]
[1] *Wolverine Tube Inc., Decatur, AL, USA*
[2] *Mechanical and Nuclear Engineering, Kansas State University, Manhattan, KS, USA*
[*] *Corresponding author. E-mail:Evraam.Gorgy@wlv.com*

The current paper presents the experimental investigation of the heat transfer performance of highly enhanced surfaced tube bundles. The two bundles studied are high pressure and low pressure TBII tubes for R-134a and R-123, respectively. The tube bundle is a staggered triangular arrangement with a tube pitch of (P/D 1.167). Twenty enhanced tubes were used in the bundle; the tube outer diameter and length are 19.05 mm (3/4 inch) and 1 m (39.36 inch), respectively. Three input variables were studied: heat flux (5-60 kW/m²), mass flux (15-55 kg/m².s), and quality (10-70%). The test saturation temperature was 4.44 ℃ for R-134a and 14.44 ℃ for R-123. The local heat transfer performance of the bundle is reported. A local method employing the Enthalpy Based Heat Transfer technique was implemented in the data reduction. Both tube bundles showed a strong dependency on heat flux as expected. The R-134a bundle showed a performance lower than that of pool boiling. The R-123 bundle showed a secondary dependency on quality. The quality effect becomes pronounced at high qualities and high average bundle heat load. In latter case enhanced tubes performance drops quickly and reaches that of a smooth tube.

Introduction

The current paper presents a study of the heat transfer performance of enhanced tube bundles. This research project was funded by ASHRAE (RP-1316). The type of analysis used in this research is based on local measurements. Specifically, four instrumented tubes included in the bundle are used to determine local heat transfer coefficients. The overall bundle was setup in a staggered arrangement of 20 tubes with a standard tube pitch (P/D 1.167). The application of this research is in design of flooded refrigerant evaporators, which have wide impact in the HVAC&R industry. A typical application for the flooded evaporators is high capacity centrifugal chillers.

A flooded evaporator is a shell and tube heat exchanger in which a fluid circulates inside the tube bundle and is cooled by a refrigerant circulating in the shell and over the tube bundle. Cooling takes place through boiling (phase change) of the refrigerant. In flooded evaporators, the refrigerant flows over the tube bundle from the bottom up; it enters the shell at a thermodynamic quality near 10%, due to the expansion device, and leaves at 100% quality

Evraam Gorgy, Ph.D., Associate Member ASHRAE is senior research engineer at Wolverine Tube Inc. and **Steven Eckels**, Ph.D., Member ASHRAE is professor at Kansas State University

(saturated vapor). This application is usually called “shell boiling.” The tubes used in these bundles can be smooth or enhanced.

The goal of the current study is to investigate the effect of heat flux, mass flux and quality on the heat transfer performance of flooded refrigerant evaporators that utilize highly enhanced tubes. This includes both high and low pressure refrigerants R-134a and R-123 and tubes designed specifically for each refrigerant. The primary outcome is the local heat transfer coefficient in the bundle. The following sections describe the facility, the data analysis used and presents the results.

The primary global variables for designing flooded refrigerant evaporators are heat duty, mass flux, tube arrangement, and tube pitch. Within the tube bundle, variables like heat flux and quality vary considerably. The test matrix was set up as a three dimensional matrix (5×6×4), where the number of points corresponds to the input variables as shown in Table 1.

Table 1 Test matrix inputs

Mass flux (kg/s.m²)	15	20	25	35	45	55
Heat flux (kW/m²)	5	15	30	45	60	
Inlet Quality	0.10	0.35	0.55	0.70		

Background

Boiling on a tube bundle has been in use for decades and has many applications: fire tube steam boilers, kettle re-boilers, waste heat boilers, and flooded refrigerant evaporators. The focus of this study is flooded refrigerant evaporators, which are widely used in centrifugal chillers, a high capacity cooling application. In flooded evaporators, refrigerant enters the tube bundle as a two phase mixture (at approximately 10% quality) due to the expansion device effect, and refrigerant typically leaves the bundle as saturated vapor. The possible heat transfer regimes of the flooded evaporator from bottom to top are as follows: convective heat transfer, sub-cooled boiling, nucleate boiling, sliding bubbles evaporation, and film boiling. In some cases, the top tubes may experience dry-out. The types of tubes used in flooded refrigerant evaporators are smooth, integral fin, and enhanced. Recently, enhanced tubes have been the focus of many research projects because of their high efficiency. Furthermore, enhanced tube technology has been on the rise as machining techniques continue to advance, previously an obstacle to developing these tubes.

Among those who provided tube bundle reviews are Ribatski and Thome (2007), Webb (2005), Casciaro and Thome (2001) Part 1, Browne and Bansal (1999), Thome (1998), Thome (1996), Collier and Thome (1996), Thome (1990), Jensen and Hsu (1988). Three variables have the most significant effect on the heat transfer coefficient (often referred to as "bundle performance"): heat flux, quality, and mass flux. Those variables are also the center of the analysis of the current study. Notably, Fujita et al. (1986), Memory et al. (1992), and Memory et al. (1994) studied boiling over smooth and enhanced tube bundles in a pool of liquid. However, this is considered a different application than that in the current study, since it does not present the effect of mass velocity on convective boiling; in some cases, the calculation of quality is not possible. Therefore, the effect of quality cannot be assessed.

The following authors reported varied enhanced tube bundle studies highlighting the effect of heat flux, quality, and mass flux. Chyu et al. (2009) studied boiling of ammonia/lubricant mixture on a horizontal enhanced tube bundle; the bundle effect was more significant at higher saturation temperatures. Also, saturation temperature had a more significant effect on the tube bundle performance than on the pool boiling performance. Schafer et al. (2007) studied the effect of novel plasma-coated tubes on the bundle performance using R-134a as the working fluid; coated tubes showed a significant increase in bundle performance and single tube performances. At higher heat fluxes, bundle performance approached that of a single tube. Chien and Wu (2004) studied convective boiling of R-123 and R-134a over smooth and low fin tube bundles. They reported that the heat transfer coefficient increased with the increase of quality for R-134a on smooth tube, while the mass flux had small effect on performance. Also, low fin tubes showed significant performance enhancement over smooth tubes.

Robinson and Thome (2004) presented one of the most comprehensive studies on this topic, studying the local bundle heat transfer coefficient (comparable to the current study) for three types of tube bundles all with standard tube pitch (P/D 1.167). For smooth tube bundles, they reported that the local heat transfer coefficient did show a significant change with the change of mass flux. Next, for a constant mass flux over a range of quality, the heat transfer coefficient increased with the increase of heat flux. However, for constant heat flux and mass flux, the heat transfer coefficient did not show a significant effect with the change of quality.

For the latter authors study of an integral fin (1024 fins/m (26 fins/inch)) tube bundle, the heat transfer coefficient did not show a significant change with the change of mass flux over a range of quality and constant heat flux while for constant mass flux and heat flux, the heat transfer coefficient did not show a significant change with the change of quality.

Also, for the enhanced tube portion of the study (Turbo BII tube), and for a range of quality and constant mass flux, the heat transfer coefficient did not show a significant change with mass flux. Again, for constant mass and heat fluxes, the heat transfer coefficient did not show a significant change with quality. Meanwhile, the bundle effect ranged from 0.8 to 1.6 for R-134a, and from 0.6 to 1.2 for R-410a and R-507a.

Kim et al. (2002) presented a study of different types of enhanced tube bundles with R-134a and R-123 at different saturation temperatures. They conducted tests for smooth tube bundles as well and reported that the heat transfer coefficient for the enhanced tube bundles was dominated by heat flux with negligible dependency on mass flux or quality. The increase in saturation temperature enhanced the heat transfer coefficient. Finally, they reported that the convective effect for R-134a was higher than for R-123 for the enhanced tubes, but the smooth tube bundle showed the opposite. They explained that this interesting phenomenon is likely due to the bubble behavior (frequency and size). For the enhanced bundle the bubble size generated at the tube pores is the same for both refrigerants, so the convective effect is dominated by bubble frequency and is higher for R-134a than R-123 regardless that the bubble size of R-123 is larger. For the smooth bundle and given the larger bubble size of R-123 and that bubbles are generated at the tube surface, the convective effect is dominated by bubble size rather than frequency and will yield higher for R-123 than R-134a.

Tatara and Payvar (2000) Parts I and II presented an experimental investigation of the effect of oil on boiling of R-123 and R-134a, respectively, on staggered pitch enhanced tube bundle and calculated the local heat transfer coefficient, they reported that the increase of oil concentration decreased tube performance. Moreover, Tatara and Payvar (1999) reported, without much emphasis on the physics of the trend, that the heat transfer coefficient increased with the increase of oil concentration when testing an integral fin (1024 fins/m (26 fins/inch)) tube bundle with R-123 and R-134a.

Gupta and Webb (1995a) conducted experiments for an integral fin (1024 fins/m (26 fins/inch)) tube bundle with P/D 1.25 for R-11 at two different saturation temperatures (4.4 and 26.7 °C). They studied the effect of convective boiling and pool boiling finding that convective boiling coefficients were twice as high as pool boiling coefficients. In Gupta and Webb (1995b), the authors used GEWA SE and Turbo B. Data showed convective behavior similar to that for pool boiling data and that the enhanced tubes' convective effect was much less than that for integral fin tubes.

Danilova and Dyundin (1972) presented experimental work for boiling of R-12 and R-22 over smooth and finned tube bundles (registering different fin geometry). They reported that for the bigger fin spacing, the effect of the number of rows of tubes was considerable. Specifically for small fin spacing, the effect of convective boiling was more pronounced.

Experimental apparatus

The experimental facility was constructed to measure the evaporation heat transfer coefficient in a bundle. The system is not a traditional vapor compression cycle. The system is driven with a positive displacement pump. The tube bundle was set up in the test section, the main component of the test facility, which is located at the highest point of the test facility. The height of the test section was set to provide the required net positive suction head (NPSH) for the refrigerant pump, which was proven to be a design constraint for R-123, since it operates at low pressure. The refrigerant leaving the test section flows to the condenser, the refrigerant pump, and completes the circuit with the pre-boiler as shown in Figure 1. The test section is water heated; in which, water circulates throughout the test section and a secondary heat exchanger (the heat source to the test section).

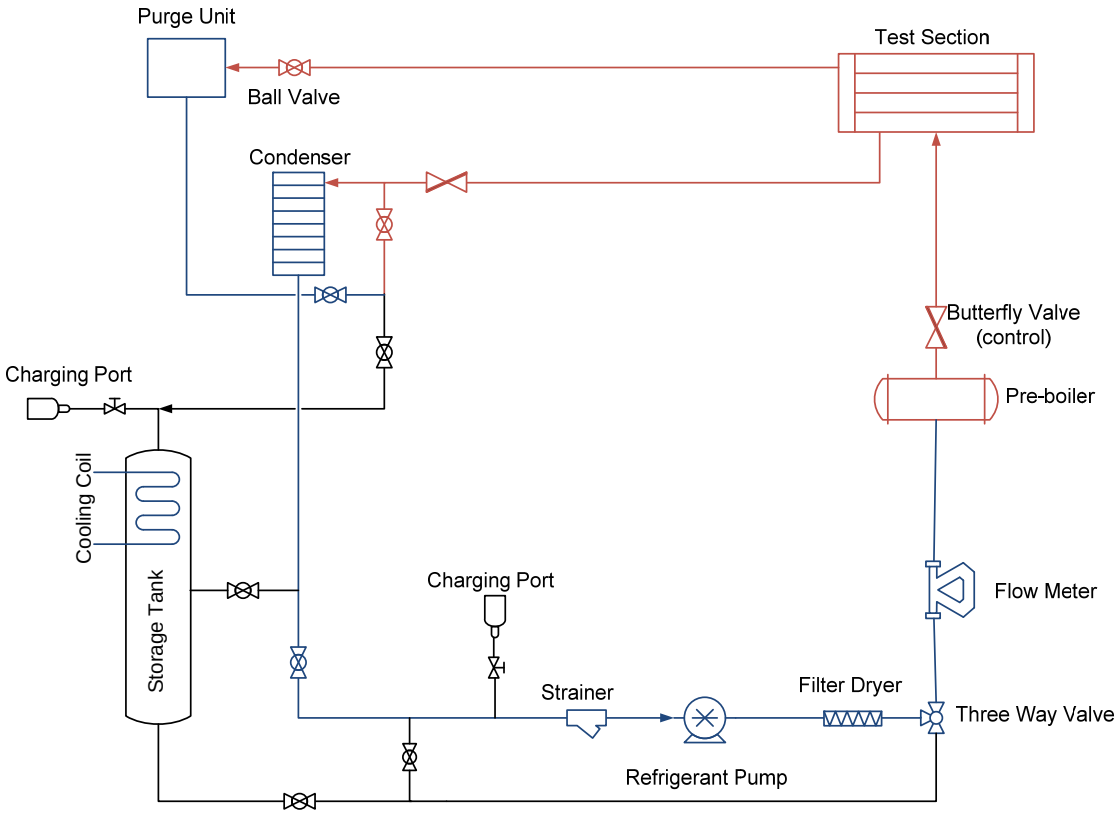

Figure 1 Schematic diagram of refrigerant circuit

Test section

The test section is a rectangular pressure vessel, designed for high and low pressure refrigerants, that is essentially a rectangular-shape shell and tube heat exchanger; the refrigerant flows up through the tube bundle while water circulates in the tubes. The test section has four sight glasses, two on each side which provided a full view of the tube bundle covering the refrigerant inlet up to the top of the tube bundle. The tubes and steel endplates are sealed together by expanding the copper tubes, which is known as tube rolling. Plates placed inside the bundle are used for mounting half dummy tubes. The half dummy tubes create symmetry for the refrigerant flow around the tubes and simulate an actual evaporator, i.e. making one side a mirror image of the other.

Refrigerant enters the tube bundle via 8 inlet ports, equally spaced along the length of the test section. The ports are aimed downward, opposite to the flow direction, to reduce the flow kinetic, thus making the vapor equally distributed. In addition, four dummy tubes having the same diameter and tube pitch as the active tubes are swaged in the endplates. Meanwhile, refrigerant exits the tube bundle through rollover rectangular openings on the sides of the test section. The total number of openings is six, three on each side.

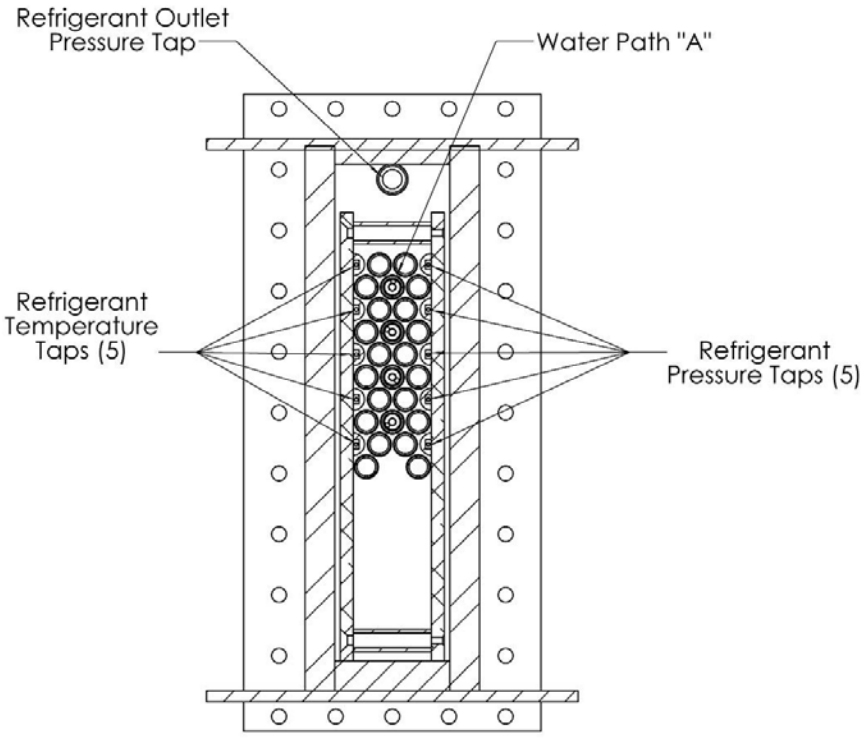

Figure 2 Test section cross sectional view

The water enters the test section at the top of the bundle and is divided into five channels (paths) parallel to each other, it is then sufficient to have the water measurements only on one of the five paths. This instrumented path was chosen to be the middle tube of the three-tube-set at each row, and was given the name "A." The water measurements include temperature and pressure measurements. Temperature drop is measured for each of the four tubes of path "A," while pressure drop is measured across the first and last tubes; that can also be used for determining the total pressure drop across the four tubes. Heat flux was adjusted in the other four paths to match that of "A."

Water instruments

Total temperature drop in path "A" is determined by measuring the temperature drop in each of the four tubes. An insert tube made of stainless steel wrapped with thick helical cable is placed in the center of each enhanced tube. The insert tube carries seven thermistors, two for measuring the inlet and outlet water temperatures and five internal thermistors for determining the local parameters. Details about the insert tube are mentioned in the next subsection. The themistors were manufactured in the lab by encapsulating each thermistor in a set screw as shown in **Error! Reference source not found.**. The set screw was drilled so that the temperature element is near the tip of the device. Once manufactured, the thermistor probes were calibrated and checked before being affixed to the insert tube. All temperature instruments were calibrated using a constant temperature bath (made by Fluke model 7321) with an uncertainty of ±0.01 °C and uniformity of ±0.005 °C. the temperature bath was calibrated using NIST traceable thermometers with a resolution of 0.01°C. The flow meters used were Coriolis type, which is known for its high accuracy.

Insert tube

The water entering the test section flows within the test tube and over the insert tube (or in between the test tube and insert tube) as illustrated in Figure 3. The insert tube has two purposes: to increase the water velocity and thus the water heat transfer coefficient, and to support the seven thermistors. The higher the water heat transfer coefficient, the more accurate the measured heat transfer coefficient will be because of the better thermal resistance balance. This is tempered by the fact that Wilson Plot can be more difficult. Two of the seven thermistors, the outermost ones, are located outside the heated section and measure the inlet and outlet temperatures of the water. These two probes are axially located in the end-plates of the test section. The advantage of this location is to

decrease any inaccuracy of the temperature measurement due to ambient loss. The other five thermistors are evenly distributed along the insert tube. The probe tip was located at the center of the space between the test tube and the insert tube and secured in position by tapping a hole in the insert tube wall and threading the probe to the require depth. The insert tube is centered inside the 1.3 m (51.5 inch) long and 0.01905 m (0.75 inch) nominally wide test tube. Dimensions of the test tubes are provided in Table 2. The tubes are externally and internally enhanced for refrigerant and water, respectively.

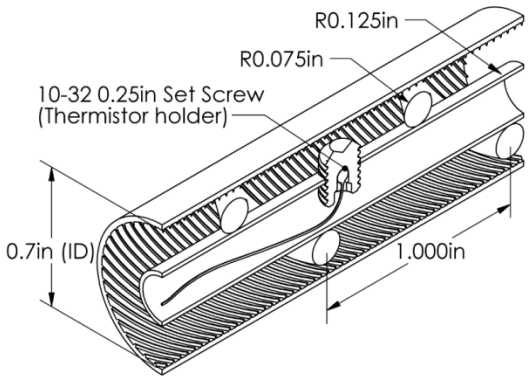

Figure 3 Cross sectional view of test tube and insert tube

Table 2 Enhanced tubes dimensions

	Outside Dia. *mm (inch)*	*Nominal Wall* *mm (inch)*	*Fin/inch*	*Finished fin OD* *mm (inch)*	*Inside Root Dia.* *mm (inch)*	*Outside Root Dia.* *mm (inch)*
TBIIHP	19.05 (0.75)	0.635 (0.025)	48	18.69 (0.736)	0.559 (0.022)	17.32 (0.682)
TBIILP	19.05 (0.75)	0.635 (0.025)	48	18.75 (0.738)	0.559 (0.022)	17.27 (0.680)

Refrigerant instruments

Temperature and pressure are measured at five levels (heights) in the shell: one at the bundle inlet and four located above the plane of the four instrumented tubes of path "A" as illustrated in Figure 2. Only pressure measurements were used in the analysis; temperature measurements were used only to check the agreement between the temperature and the corresponding saturation temperature determined from the pressure transducers' measurement (± 0.2 °C was considered acceptable). Temperature probes and pressure transducers are connected to the half dummy tubes installed on the test section's inside plates. Each refrigerant has its own set of pressure transducers, high-range pressure transducers for R-134a and low-range pressure transducers for R-123 for increased accuracy. Refrigerant flow rate was measured using a Coriolis type flow meter.

Data reduction

Tube bundle heat transfer performance is evaluated over a range of heat fluxes, mass fluxes, and other qualities. Particularly, the heat transfer coefficients reported in this study are local to one location in the bundle. The water temperature is measured at five locations in each of the four tubes of the instrumented water path. This data is fit with a second degree polynomial as $T = f(z)$. A finite heat transfer analysis determines the local heat transfer coefficient. Heat is transferred from the water to the cylinder's inner wall by convection, from the inner wall to its outer wall by conduction, and from the outer wall to the refrigerant by convection.

Consequently, applying conservation of energy and the 1-D heat transfer equations on the finite control volume, assuming no fouling resistance, yields

$$h_w dA_i \left(T_{hot} - T_{wall,in}\right) = \frac{2\pi k_c dz}{\ln\left(\frac{D_o}{D_i}\right)}\left(T_{wall,in} - T_{wall,out}\right) \equiv dQ \tag{1}$$

and

$$h_r dA_o \left(T_{wall,out} - T_{cold}\right) = \frac{2\pi k_c dz}{\ln\left(\frac{D_o}{D_i}\right)}\left(T_{wall,in} - T_{wall,out}\right) \equiv dQ \tag{2}$$

where

$$dA_i = \pi D_i dz\,, \tag{3}$$

and

$$dA_o = \pi D_o dz\,. \tag{4}$$

Applying Newton's law of cooling yields

$$dQ = U \cdot dA_o \left(T_{hot} - T_{cold}\right). \tag{5}$$

Defining the thermal resistance of the tube wall as

$$R_{wall} = \frac{1}{2\pi dz k_c}\ln\left(\frac{D_o}{D_i}\right). \tag{6}$$

Using Equations (1), (2), (5), and (6), yields the following thermal resistances model

$$\frac{1}{UdA_o} = \frac{1}{h_w dA_i} + \frac{1}{2\pi dz k_c}\ln\left(\frac{D_o}{D_i}\right) + \frac{1}{h_r dA_o}\,. \tag{7}$$

Substituting Equations (3) and (4) yields

$$\frac{1}{U} = \frac{1}{h_w}\frac{D_o}{D_i} + R'_{wall} + \frac{1}{h_r}. \tag{8}$$

Solving for the heat transfer coefficient h_r yields

$$h_r = \left(\frac{1}{U} - R'_{wall} - \frac{1}{h_w}\frac{D_o}{D_i} \right)^{-1}. \tag{9}$$

Local heat transfer coefficient

Notably, Equation (9) is length independent. Therefore, all the variables of Equation (9) can be used in the local or average analysis (for example, U_{lcoal} or U_o). To determine the local heat transfer coefficient, Equation (9) is modified to

$$h_{local} = \left(\frac{1}{U_{local}} - R'_{wall} - \frac{1}{h_w}\frac{D_o}{D_i} \right)^{-1}, \tag{10}$$

where U_{local} is the local overall heat transfer coefficient. Following the definition of Newton's law of cooling yields

$$U_{local} = \frac{q''_{local}}{T_{local} - T_\infty}. \tag{11}$$

Substituting in Equation (10) yields

$$h_{local} = \left(\frac{T_{local} - T_\infty}{q''_{local}} - R'_{wall} - \frac{1}{h_w}\frac{D_o}{D_i} \right)^{-1}. \tag{12}$$

As stated in Equation(12), the local heat transfer coefficient is determined at each local temperature measurement.

Local heat flux

The total heat transfer is determined according to the Enthalpy Based Heat Transfer Analysis (EBHT), which accounts for the effect of pressure change. For the current configuration, the water flow inside the tube experiences large pressure drop. In Equation (12), the local temperature T_{local} and refrigerant temperature T_∞ are obtained by direct measurements while the local heat flux q''_{local} is determined by the enthalpy change on the differential element as

$$dQ = \dot{m} \cdot di. \tag{13}$$

Assuming incompressible fluid (valid for the current water operating conditions), the finite enthalpy di can be expressed as

$$di = C_p \cdot dT + v \cdot dP \ . \tag{14}$$

Substituting in Equation (13) and dividing by $\pi \cdot D_o \cdot dz$ yields

$$\underbrace{\frac{dQ}{\pi dz D_o}}_{q''_{local}} = \frac{\dot{m}}{\pi D_o}\left(C_p \frac{dT}{dz} + v \frac{dP}{dz} \right). \tag{15}$$

where dT/dz is determined from

$$T = C_1 z^2 + C_2 z + C_3 . \tag{16}$$

The pressure drop term of Equation (15) can be determined by assuming a linear water pressure drop across the tube since the pressure can be determined at the inlet and outlet of each tube. Therefore, dP/dz is reduced to $\Delta P/L$. Pressure drop and temperature slope are determined according to the tube length (1 m). The last necessary component in Equation (12) is the water heat transfer coefficient.

Water heat transfer coefficient

The water flows between the enhanced tube and the insert tube following the swirl shape of the insert tube as illustrated in Figure 3. For flow inside a tube, the heat transfer coefficient for no phase change can be determined using

$$h_i = \frac{Nu_D \cdot k_w}{D_h}, \tag{17}$$

where all the water properties are evaluated at the average inlet and outlet temperatures. For this study the water side Reynolds number varied from 10,000 to 35,000. Since the flow is exclusively turbulent, the Nusselt number can be determined using Gnielinski's correlation (1976) presented as

$$Nu_D = \frac{(f/8)(\mathrm{Re}_D - 1000)\mathrm{Pr}}{1 + 12.7(f/8)^{1/2}\left(\mathrm{Pr}^{2/3} - 1\right)}. \tag{18}$$

The entrance region can be ignored because of the presence of the swirls and the turbulent flow. The above correlation, also called the modified Petukhov's correlation (1970), is widely applied in flow inside tubes; Gnielinski's correlation works over a wide range of Reynolds numbers (3000 to 5×10^6) and Prandtl numbers (0.5 to 2000) with accurate results, the friction factor is defined as

$$f = \left(0.79 \ln\left(\mathrm{Re}_D\right) - 1.64\right)^{-2}. \tag{19}$$

The friction factor proposed by Gnielinski in Equation (19) is that of a smooth tube. Since the tubes used are internally enhanced and the pressure drop is measured over each tube, the friction factor can be calculated directly rather than depending on a model

$$f = \frac{\Delta P}{\rho} \cdot \frac{D_h}{L_c} \cdot \frac{2}{V^2}. \tag{20}$$

The internal enhancement of the tubes (micro-fins) and the insert tube's swirls affect accuracy in measuring both the characteristic length and the hydraulic diameter of the above equation. Therefore, the Gnielinski correlation needs a correction factor multiplier, which is determined using the modified Wilson plot technique (Briggs and Young (1969)). Accordingly, the correction factor becomes the leading coefficient of the water heat transfer coefficient as

$$h_w = C_i \cdot h_i. \tag{21}$$

The modified Wilson plot technique was done in a single tube test section as a part of the pool boiling study of this project. Details were published earlier in Gorgy and Eckels (2010) and Gorgy and Eckels (2012). The uncertainty in the water side heat transfer coefficient was dominated by the uncertainty in C_i which was found from the 95% confidence interval of the linear regression.

Local quality

Similar to the local heat transfer coefficient, the local quality is determined at each temperature measurement location (thermistor) and at the minimum flow area between the tubes. The thermodynamic quality is determined by performing an energy balance between the refrigerant side and the water side as

$$\dot{m}_{ref} \cdot \Delta x \cdot h_{fg} = q''_{local} \cdot \pi DL. \tag{22}$$

The test section's 1 m side is theoretically divided into four horizontal planes and five vertical sections, producing 20 control volumes. The test section then becomes a (4×5) matrix. Above each plane (row) lies a group of five tubes; the vertical sections (columns) divide the test section so that the thermistors are centered in each vertical section. Therefore, applying the energy balance on each control volume yields

$$\frac{\dot{m}_{ref}}{5} \cdot \underbrace{\Delta x}_{\left(x_{i+1,j} - x_{i,j}\right)} \cdot h_{fg} = 5 \cdot q''_{local_{i,j}} \pi D \frac{L}{5}, \tag{23}$$

or

$$x_{i+1,j} = \frac{5q''_{local_{i,j}} \cdot \pi DL}{\dot{m}_{ref} \cdot h_{fg}} + x_{i,j}\,. \tag{24}$$

Since the quality at the bundle bottom is constant at all five locations and equals the test section inlet quality, the quality at each row is determined from the bottom up. The subscript i, j corresponds to (row,column); with the quality at row i and the local heat flux $q''_{local_{i,j}}$, the quality at the next row $i+1$ is determined. The local quality (the quality at the minimum cross-sectional area) is calculated by adding the quality entering the instrumented tube to the quality rise due to the local heat flux at the tube centerline. The latter quality is determined by performing an energy balance around the instrumented tube which is in the center of three tubes (i.e. within each of the 20 control volumes). Thus, the energy balance can be expressed as

$$\frac{\dot{m}_{ref}/5}{3} \cdot \underbrace{\Delta x}_{\left(x_{local_{i,j}} - x_{i,j}\right)} \cdot h_{fg} = \frac{q''_{local}}{2} \cdot \pi D \frac{L}{5}, \tag{25}$$

or

$$x_{local_{i,j}} = \frac{q''_{local}/2 \cdot \pi DL}{\dot{m}_{ref}/3 \cdot h_{fg}} + x_{i,j}\,. \tag{26}$$

Mass flux

The mass flux (also called mass velocity) is calculated based on the minimum area between tubes as

$$G = \dot{m}/A_{\min}\,, \tag{27}$$

where

$$A_{\min,P/D} = \left(\left(P/D\right) \times D - D\right)\left(L_T\right)\ \mathrm{m}^2\,. \tag{28}$$

Uncertainty analysis

The uncertainty analysis is performed using the Kline-McClintock (1953) second order law. To determine the final uncertainty in the heat transfer coefficient first required defining the input variables uncertainty. The input variables can be the measured variables (temperature, pressure, and flow rate) or the calculated variables such as saturation temperatures, water heat transfer coefficient, and so forth. Table 3 presents the input uncertainties. The water properties were called in Excel from RefProp 8.0 without using curve fit equations. Therefore, the water properties uncertainty is considered negligible.

Table 3 Input Uncertainty

u_T(°C/°F)	±0.015/0.027	u_m	± 0.1% × Reading	$u_{wp,low\text{-}range}$	±0.5157l kPa/0.075 PSI
$u_{Tsat,\ R134a}$(°C/°F)	±0.022/0.0369	$u_{wp,high\text{-}range}$	± 1.0342 kPa/0.15 PSI	u_{hw}	$0.04 \cdot h_w$
$u_{Tsat,\ R123}$(°C/°F)	±0.03/0.054				

The local heat transfer coefficient is determined by applying propagation of error on Equation (29). The uncertainty in all the variables in this equation is given in **Error! Reference source not found.**, except the local temperature T_{local} and the temperature slope dT/dz. The temperature slope uncertainty was determined using a Monte Carlo simulation which is explained at length in Gorgy and Eckels (2012). The uncertainty of the local temperature is the same as the temperature uncertainty. The analysis showed that the dominant source of uncertainty is the temperature uncertainty; therefore, data at low heat flux presents higher uncertainty than high heat flux data because of the low temperature difference.

$$h_{local} = \left(\frac{T_{local} - T_{sat}}{\dot{m} / \pi D_o \left(C_p \left| dT/dz \right| + v \Delta P / L \right)} - R'_{wall} - \frac{1}{h_w} \frac{D_o}{D_i} \right)^{-1} . \tag{29}$$

R-134a results

Data points are sorted according to heat flux, mass flux and local quality. Those three variables are interrelated, which makes it difficult to determine the change in the heat transfer coefficient with respect to one variable independent of the other two (i.e. the other two held constant). Rather, the range of the other two variables is kept as narrow as possible. Next, the bundles' heat transfer coefficient vs. heat flux plots often includes the single pool boiling curve for comparing the convective and pool boiling for each tube pitch. Ultimately, heat flux proves to be the most influential variable for enhanced tubes rather than mass flux or quality; therefore, the first and most indicative plot of the bundle performance is the heat transfer coefficient vs. heat flux.

Testing was performed at a saturation temperature of 4.44 °C using an enhanced TBIIHP tube. Data were collected according to the proposed test matrix based on a total of 55 runs. Each run produces 20 data points of local heat transfer coefficients, local heat fluxes, and local qualities, thus, 1100 total data points. Figure 4 presents all 1100 points. It is clear from this figure that at low and high heat fluxes, the effect of quality and mass flux is secondary. Also, between heat fluxes of 20 and 40 kW/m², the heat transfer coefficient can vary by up to 10000

W/m².°C indicating that quality and mass flux effect are also important variables. Since heat flux is important in all three regions we consider it the dominant variable. The data is compared to that of the single tube pool boiling of the TBIIHP tube (see Gorgy and Eckels (2010) for details). At low heat flux range (minimum heat flux up to 20 kW/m²), all points show enhanced performance, which can be interpreted as the effect of early pores activation due to flow boiling. As heat flux increases, the bundle performance becomes significantly lower than does the single tube performance.

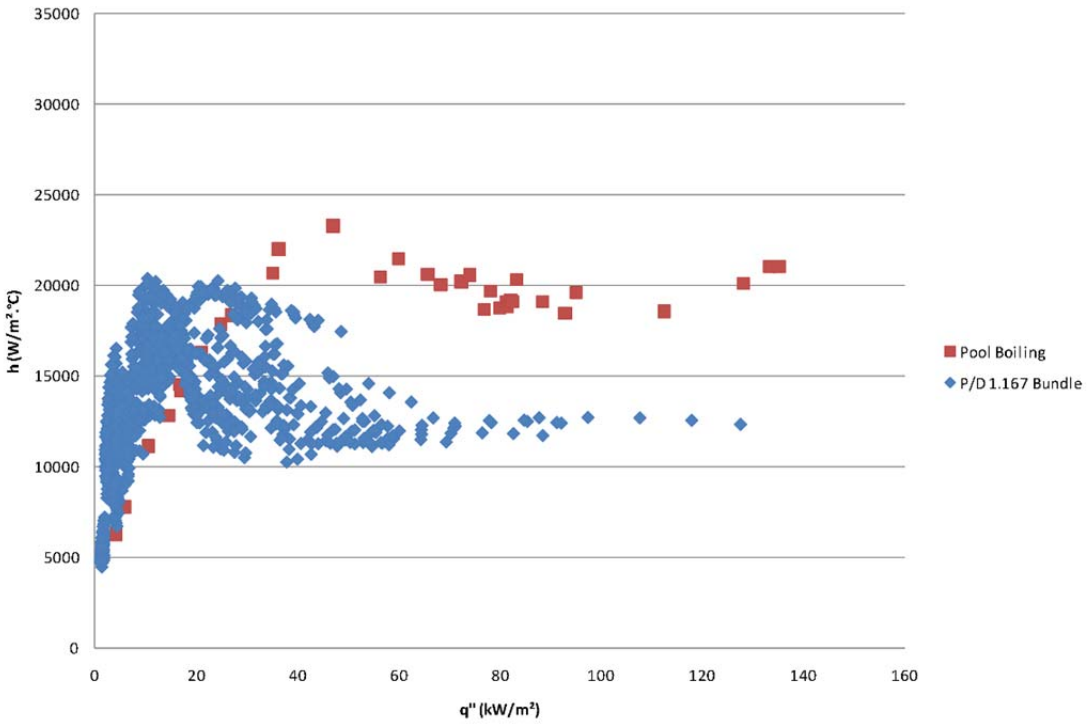

Figure 4 R-134a P/D 1.167 all data

The data presented were sorted by quality as shown in Figure 5. Data points of a quality at 10% and 20% show enhanced performance relative to the pool boiling at low heat flux, which increases with the increase in quality. Some points of the 55-60% quality range show twice the performance of the single tube in pool boiling, while all the points above the 20 kW/m² mark show a much lower performance than does the single tube. This performance deterioration reaches 50% at the 55-60% quality points range. Also, at higher heat fluxes, the higher the quality, the lower the performance. Next, all the points above 10 kW/m² show a decreasing trend with the increase of heat flux.

Finally, at 60 kW/m² and above, the heat transfer coefficient does not show a significant change with the increase in heat flux.

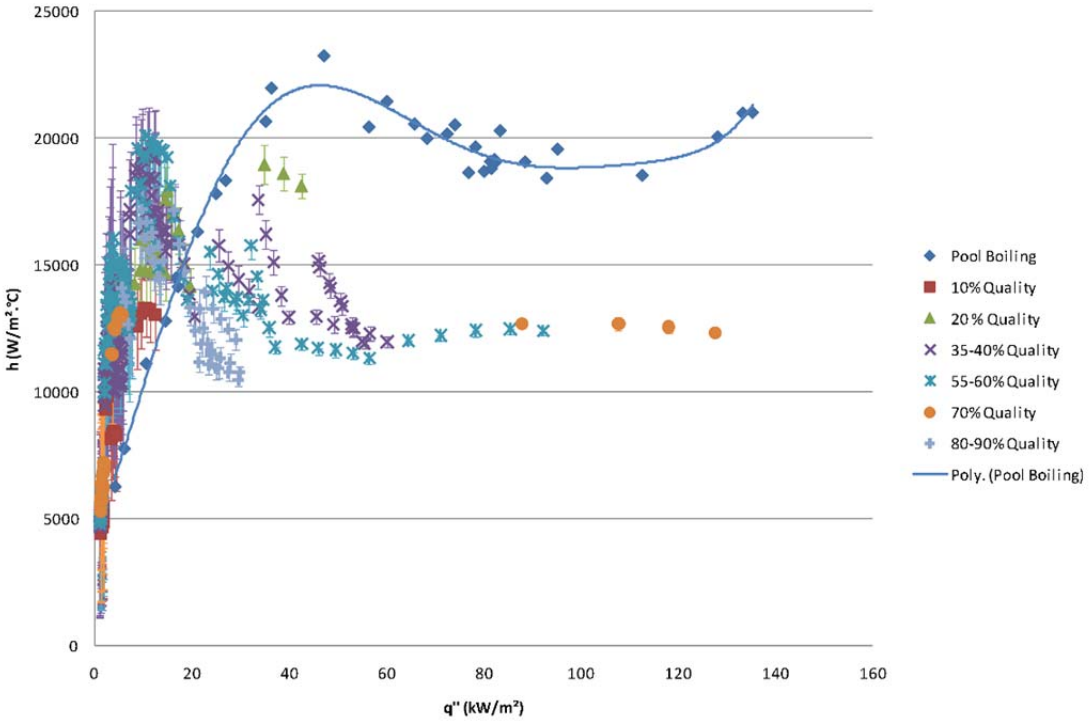

Figure 5 R-134a P/D 1.167 all data sorted by quality

Mass flux and heat flux effects

The mass flux effect can be studied by plotting the heat transfer coefficient vs. heat flux for narrow ranges of quality. Figure 6 present the heat transfer coefficient trend for different mass fluxes and for 70-85% quality (low-quality plots follow the same pattern); taking into account the heat transfer coefficient uncertainty, hardly any change occurs in the heat transfer coefficient with mass flux at the same heat flux. Therefore, the mass flux does not significantly affect performance. On the other hand, the heat flux effect is dominant.

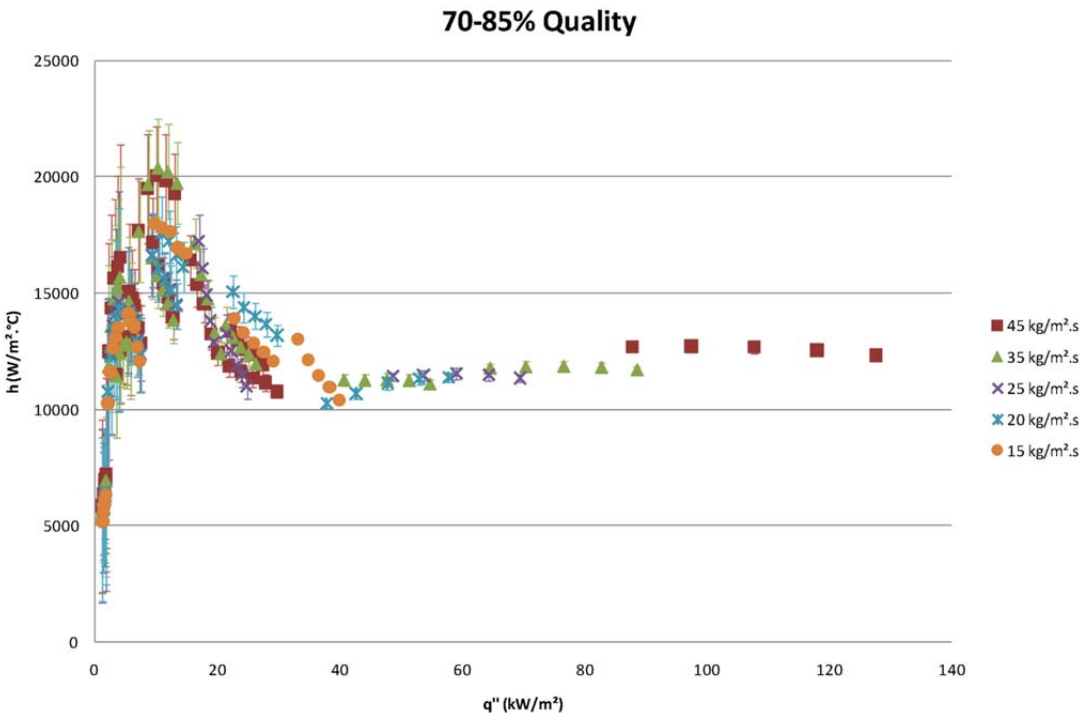

Figure 6 R-134a P/D 1.167 effect of heat flux 70-85% quality

Quality effect

For the effect of quality on the bundle performance, the heat transfer coefficient was plotted against quality for each mass flux point of the test matrix over a narrow range of heat flux points. In Figure 7, the heat transfer coefficient shows an increasing trend with the increase in quality for the 4-5 and 10 kW/m². For higher heat fluxes, the heat transfer coefficient slightly decreases with the increase in quality. The fact that the heat transfer coefficient vs. quality trends are similar at all mass flux points reinforces the conclusion that the effect of mass flux is insignificant.

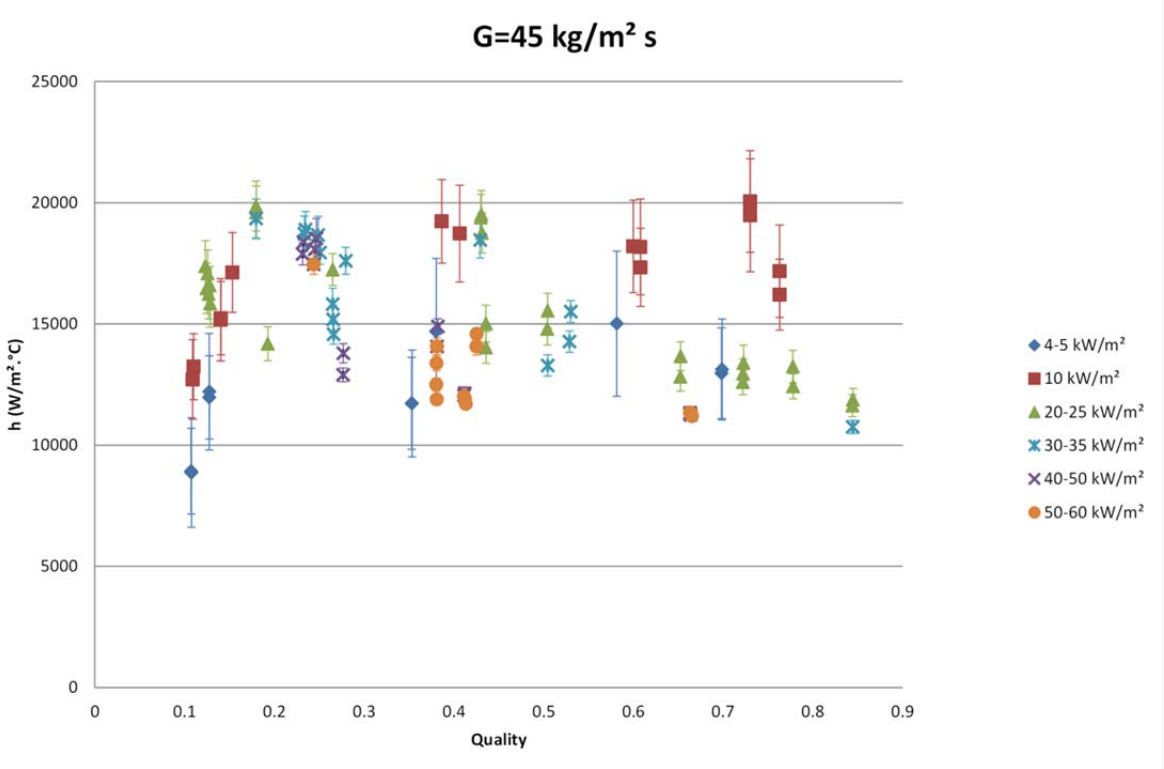

Figure 7 R-134a P/D 1.167 effect of quality at 45 kg/m².s

R-123 results

Most of the testing for R-123 was performed at a saturation temperature of 14.44 °C. Originally, the desired saturation temperature was 4.44 °C as is the case for R-134a tests, but the current test facility's configuration has a limited range of high heat fluxes and mass fluxes at 4.44 °C for R-123 (since the specific volume of R-123 vapor at 4.44 °C is 1.5 times at 14.44 °C); moreover, data taken at 4.44 °C were limited to low heat flux and mass flux. No significant difference between the two saturation temperatures was noticed, which is also clear in Figure 9. The enhanced tube used with R-123 is the TBIILP. Data were collected according to the proposed test matrix based on a total of 23 runs. Data are also compared to that of the single tube pool boiling of the TBIILP tube as shown in Figure 8. At low heat flux range (minimum heat flux up to 30 kW/m²), all points show enhanced performance due to convective boiling. Moreover, as heat flux increases, bundle performance becomes lower than that of the single tube performance, with some points experiencing a sharp decline.

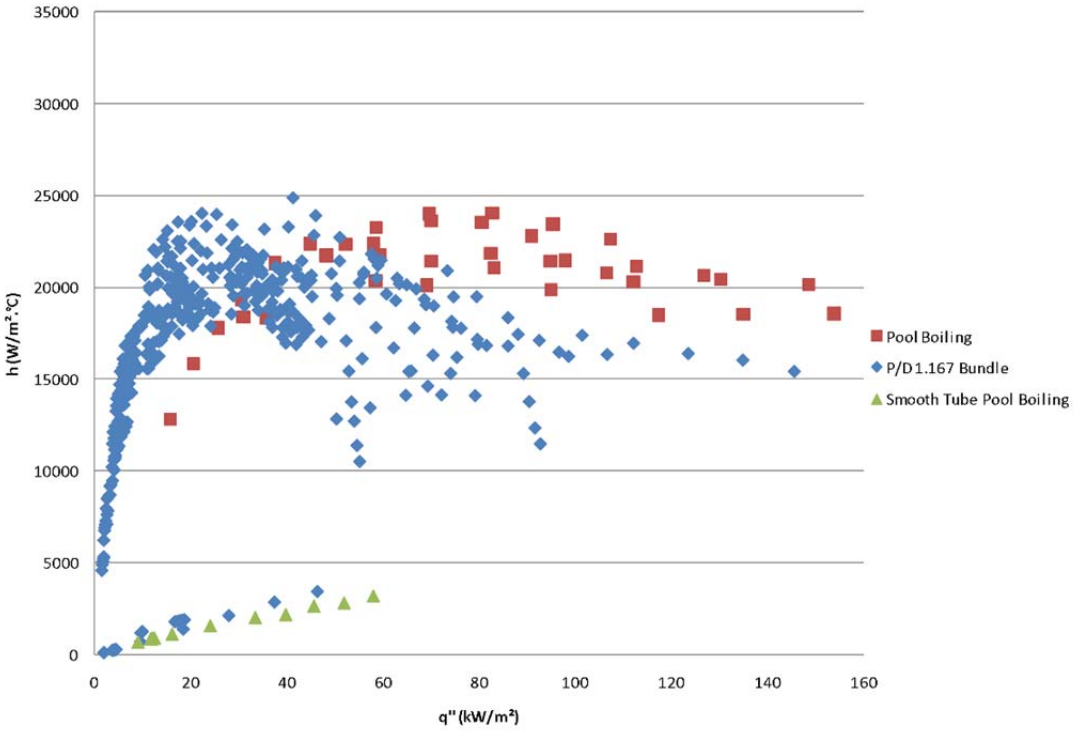

Figure 8 R-123 P/D 1.167 all data

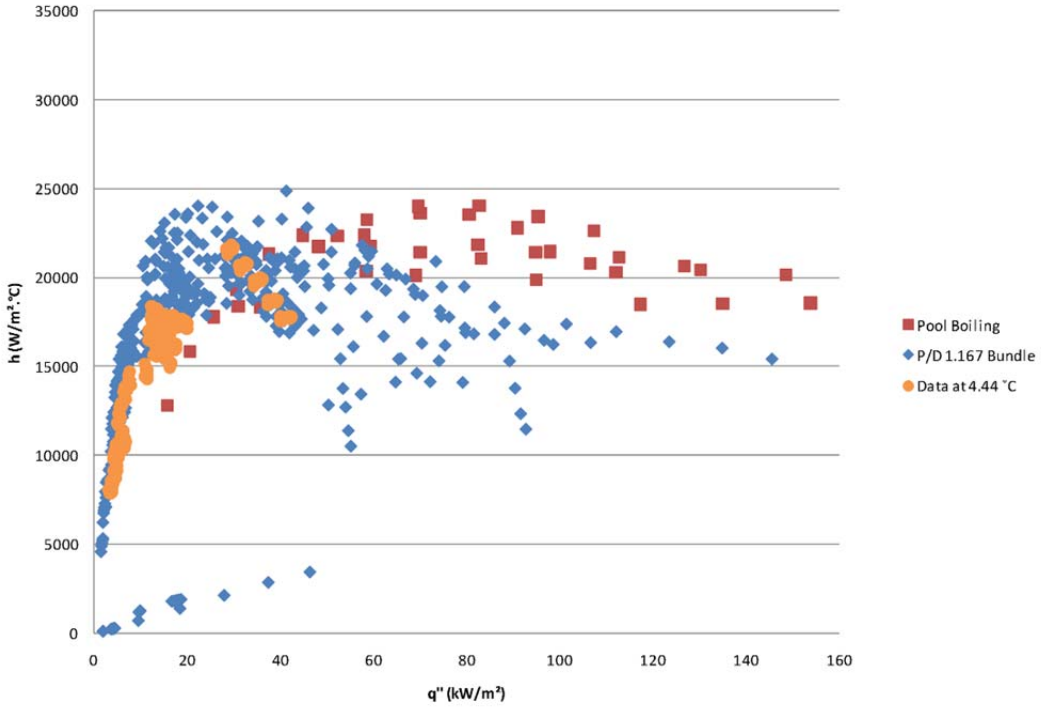

Figure 9 R-123 P/D 1.167 saturation temperature comparison

The data presented on the previous page were sorted by quality as shown in Figure 10. At low heat flux, all qualities show enhanced performance compared to that of the single tube, while at 50% quality and beyond, performance declines and deteriorates; meanwhile, all the points above 30 kW/m² show a decreasing trend with increase in heat flux. The points for 50-80% quality at the bottom of the curve show performance similar to that of a smooth tube (see also Figure 8); their heat transfer coefficient is much lower than that of other points that share the same heat flux and quality. For more details on smooth tube performance, refer to Gorgy and Eckels (2010).

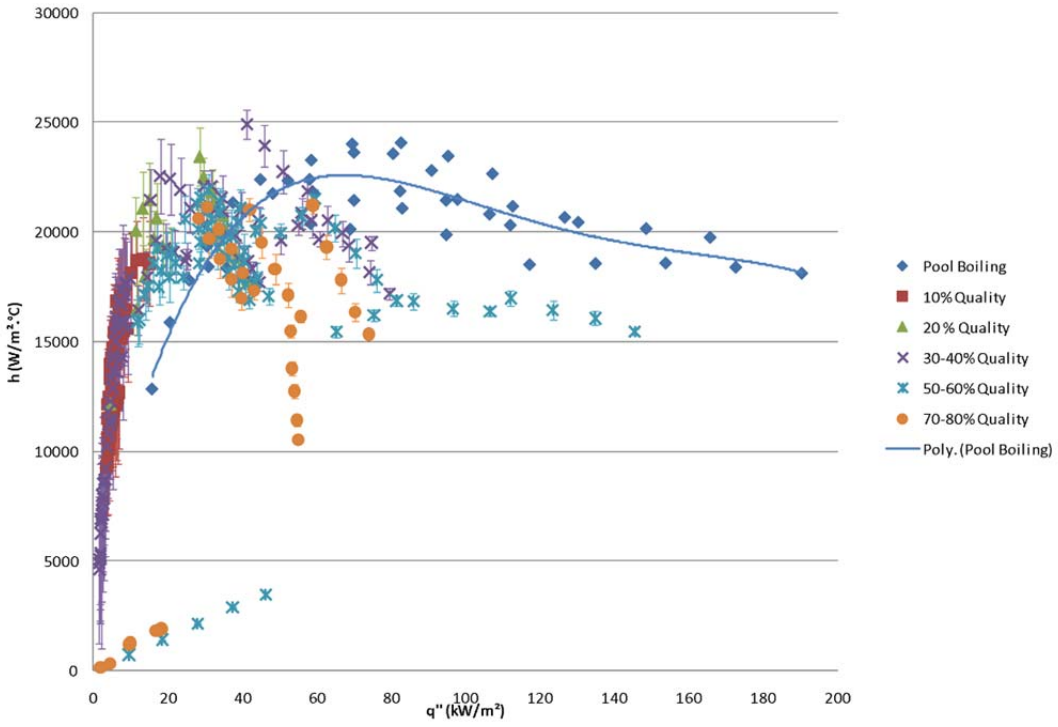

Figure 10 R-123 P/D 1.167 all data sorted by quality

Mass flux and heat flux effects

In Figure 11 (50-60% quality), and taking into account the heat transfer coefficient uncertainty, hardly any change in the heat transfer coefficient registers for mass flux at the same heat flux. However, some points show that mass flux has an effect on the heat transfer coefficient, for as the mass flux increases, the heat transfer coefficient drops quickly. These trends (including the trends presented in Figure 10) show that the heat transfer coefficient is dependent on heat flux, average bundle heat flux, and flow pattern. The dependency on flow pattern can be interpreted from the high quality points which show that for the same heat flux, two different values for the heat transfer coefficient exist. Those local points are located at the top of the bundle, suggesting that this effect is due to

flow pattern (spray flow). This phenomenon occurs at high wall superheat $\left(T_{wall} - T_{sat}\right)$ and high bundle-average heat flux, so as the bundle average heat flux increases, the top of the tube bundle (at the water inlet) experiences tube enhancement dry-out at which point the water temperature difference becomes small; hence the low local heat flux of those points. This phenomenon was also reported in Arshad and Thome (1983). This causes the enhanced tube performance to revert to that of a smooth tube.

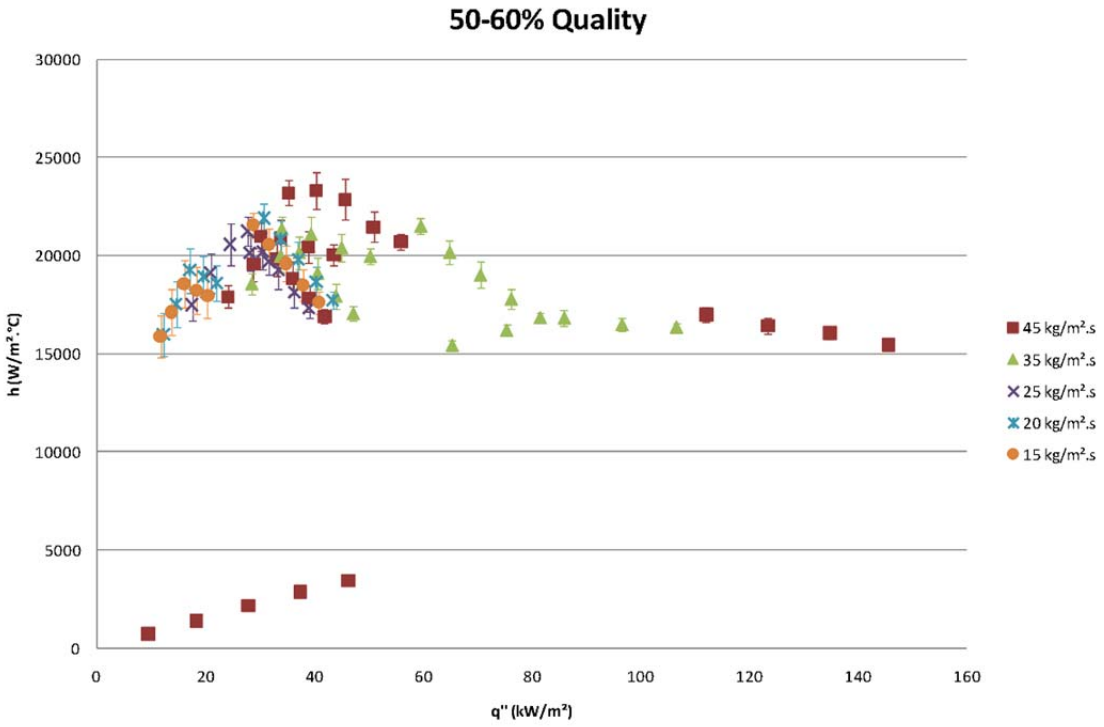

Figure 11 R-123 P/D 1.167 effect of heat flux at 50-60% quality

Quality effect

The following plot (Figure 12) presents the heat transfer coefficient vs. quality for one mass flux point of the test matrix over a narrow range of heat flux points in which the heat transfer coefficient experiences a sharp decrease at 50% quality and higher. Therefore, the heat transfer coefficient shows a strong dependency on quality at high mass fluxes. It also demonstrates that the heat transfer coefficient shows a slight increase with quality up to 50%, then sharply declines at higher qualities.

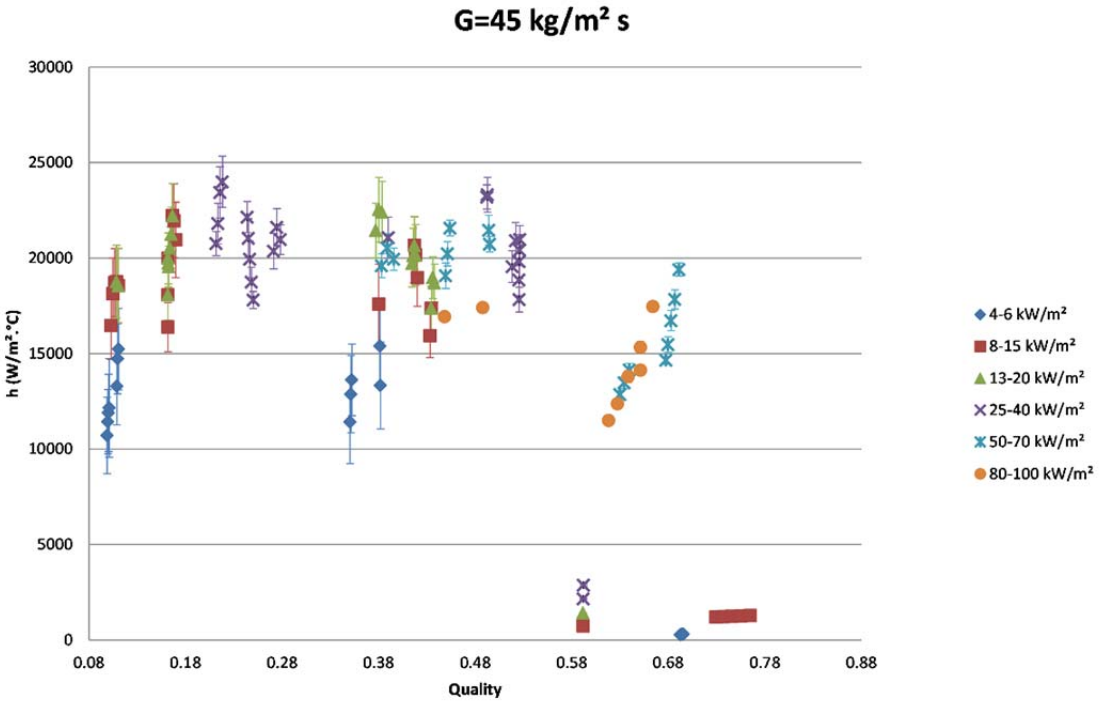

Figure 12 R-123 P/D 1.167 effect of quality at 45 kg/m².s

Conclusions

This paper presented the experimental local heat transfer coefficient results from testing shell side boiling of R-134a and R-123 over an enhanced tube bundle using TBIIHP and TBIILP tubes, respectively, with a standard tube pitch (P/D 1.167). The analysis used is local to one location in the bundle. Measurements were determined at the minimum flow area between the tubes. This investigation reported accurate boiling curves along with a clear presentation for the effect of heat flux, mass flux, and quality on the bundle performance. The results of each tube bundle showed that the dominant parameter in the bundle performance is heat flux. For the R-134a bundle, the heat transfer coefficient increases with the increase in quality at low heat flux.

While both bundles presented a rapid increase of performance at low heat flux, in comparison to pool boiling, the R-134a bundle showed a significantly lower performance than pool boiling. Evidently, the peak of the pool boiling curve exists in bundle boiling as well, but is shifted to the left; i.e. the curve peaks at a lower heat flux for convective boiling.

For the R-123 bundle, the effect of quality is apparent only at certain flow rates and high qualities. The flow pattern effect is noticeable for the points with two different values for the heat transfer coefficient for the same heat

flux, mass flux, and quality. Remarkably, the R-123 bundle experiences a drop in performance at high qualities to that of a smooth tube which is at high qualities.

Acknowledgement

This project was sponsored by ASHRAE as RP-1316 “Experimental Evaluation of Heat Transfer Impacts of Tube Pitch in a Highly Enhanced Surface Tube Bundle”. TC 8.5 monitored the program under the chairmanship of Petur Thors. Test tubes were donated by Wolverine Tube, Inc.

Nomenclature

A	Area	P	Pressure
C	Constant	P/D	Pitch to diameter ratio
C_i	Internal correction factor	Pr	Prandtl number
C_p	Specific heat at constant pressure	q''	Heat flux
D	Diameter	Q	Total heat transfer
D_h	Hydraulic diameter	ρ	Density
f	Friction factor	Re	Reynolds number
G	Mass flux	R_{wall}	Wall thermal resistance
h	Heat transfer coefficient	R'_{wall}	$dA_o \cdot R_{wall}$
h_{fg}	Specific heat of vaporization	T	Temperature
i	Enthalpy	T_{sat}	Saturation temperature
k	Thermal conductivity	T_∞	Fluid temperature
k_c	Copper thermal conductivity	U	Overall heat transfer coefficient
L	Length	u	Uncertainty
L_c	Characteristic length	v	Specific volume
$\dot{m}$	Mass flow rate	x	Quality
Nu	Nusselt number		

References

Arshad, J., and J.R. Thome. 1983. Enhanced boiling surfaces: Heat transfer mechanism and mixture boiling. *Proceedings of ASME-JSME Therm. Eng. Joint Conf* 1:191-197.

Browne, M., and P. Bansal. 1999. Heat transfer characteristics of boiling phenomenon in flooded refrigerant evaporators. *Applied Thermal Engineering* 19(6):595-624.

Briggs, D.E., and E.H. Young. 1969. Modified Wilson plot techniques for obtaining heat transfer correlations for shell and tube heat exchangers. *Chemical Engineering Progress Symposium Series* 92(65):35-45.
Casciaro, S., and J.R. Thome. 2001. Thermal performance of flooded evaporators, part 1: Review of boiling heat transfer studies. *ASHRAE Transactions* 107:903-918.
Chien, L.H., and J.S. Wu. 2004. Convective evaporation on plain tube and low-fin tube banks using R-123 and R-134a. *Transactions of ASHRAE* 110 (1): 101-8.
Chyu, M.C., et al. 2009. Bundle effect of ammonia/lubricant mixture boiling on a horizontal bundle with enhanced tubing and inlet quality. *International Journal of Refrigeration* 32(8):1876-85.
Collier, J.G., and J.R. Thome. 1996. *Convective boiling and condensation*, 3rd Ed. Oxford University Press, USA.
Danilova, G., and V. Dyundin. 1972. Heat transfer with freons 12 and 22 boiling at bundles of finned tubes. *Heat Transfer: Soviet Research* 4(4):48-54.
Fujita, Y., H. Ohta, S. Hidaka, and K. Nishikawa. 1986. Nucleate boiling heat transfer on horizontal tubes in bundles. *Proceedings of the 8th Int. Heat Transfer Conference* 5:2131-2136.
Gorgy, E.I., and S. Eckels. Average heat transfer coefficient for pool boiling of R-134a and R-123 on smooth and enhanced tubes (RP-1316). *HVAC&R* 16(5): 657-676.
Gorgy, E.I., and S. Eckels. Local heat transfer coefficient for pool boiling of R-134a and R-123 on smooth and enhanced tubes. *International Journal for Heat and Mass Transfer* 55(11-12): 2751-3326.
Gnielinski, V. 1976. New equations for heat and mass transfer in turbulent pipe and channel flow. *Int.Chem.Eng* 16(2):359-68.
Gupte, N.S., and R.L. Webb. 1995. Shell-side boiling in flooded refrigerant evaporators part I: Integral finned tubes. *HVAC and R Research* 1(1):35-47.
Gupte, N.S., and R.L. Webb. 1995. Shell-side boiling in flooded refrigerant evaporators part II: Enhanced tubes. *HVAC and R Research* 1(1):48-60.
Jensen, M., and J.T. Hsu. 1988. A parametric study of boiling heat transfer in a horizontal tube bundle. *Journal of Heat Transfer* 110:976.
Kim, N.H., et al. 2002. Forced convective boiling of pure refrigerants in a bundle of enhanced tubes having pores and connecting gaps. *International Journal of Heat and Mass Transfer* 45(12):2449-63.
Kline, S.J., and F. McClintock. 1953. Describing uncertainties in single-sample experiments. *Mechanical Engineering* 75(1):3-8.
Memory, S., et al. 1994. Nucleate pool boiling of a TURBO-B bundle in R-113. *Journal of Heat Transfer* 116(3):670-8.
Memory, S.B., SV Chilman, and PJ Marto. 1992. Nucleate boiling characteristics of a small enhanced tube bundle in a pool of R-113. *28th National Heat Transfer Conference and Exhibition* 129-138.
Petukhov, B. 1970. Heat transfer and friction in turbulent pipe flow with variable physical properties. *Advances in Heat Transfer* 6:503-64.
Ribatski, G., and J.R. Thome. 2007. Two-phase flow and heat transfer across horizontal tube bundles-a review. *Heat Transfer Engineering* 28(6):508-24.
Robinson, D.M., and J. Thome. 2004. Local bundle boiling heat transfer coefficients on a integral finned tube bundle (RP-1089). *HVAC and R Research* 10(3):331-44.
Robinson, D.M., and J.R. Thome. 2004. Local bundle boiling heat transfer coefficients on a plain tube bundle (RP-1089). *HVAC and R Research* 10(1):33-51.
Robinson, D.M., and J.R. Thome. 2004. Local bundle boiling heat transfer coefficients on a turbo-BII HP tube bundle (RP-1089). *HVAC and R Research* 10(4):441-57.
Schäfer, D., et al. 2007. The effect of novel plasma-coated compact tube bundles on pool boiling. *Heat Transfer Engineering* 28(1):19-24.
Tatara, R.A., and P. Payvar. 2000. Effects of oil on boiling of replacement refrigerants flowing normal to a tube bundle - part I: R-123. *Proceedings of ASHRAE Winter Meeting* 106.
Tatara, R.A., and P. Payvar. 2000. Effects of oil on boiling of replacement refrigerants flowing normal to a tube bundle - part II: R-134a. *Proceedings of ASHRAE Winter Meeting* 106.
Tatara, R.A., and P. Payvar. 1999. Effects of oil on boiling R-123 and R-134a flowing normal to an integral-finned tube bundle. *ASHRAE Transactions* 105.
Thome, J.R. 1996. Boiling of new refrigerants: A state-of-the-art review. *International Journal of Refrigeration* 19(7): 435-57.
Thome, J. 1998. Boiling and evaporation of fluorocarbon and other refrigerants: A state-of-the-art review. *Air-Conditioning and Refrigeration Institute (ARI), Arlington, Virginia.*
Webb, R.L., and N-H Kim. 2005. *Principles of enhanced heat transfer*, 2nd Ed. Taylor & Francis, LLC